

Discontinuous Palladium Nanostructures for H₂ Sensing

C.Fournier^c, T. Kiefer^a, G. Villanueva^a, F. Fargier^c, R.M. Penner^b, J. Brugger^a, and
F. Favier^c

^a Microsystems Laboratory, Station 17, Ecole Polytechnique Federale de Lausanne
(EPFL), Lausanne, 1015, Switzerland

^b Department of Chemistry, University of California Irvine, Irvine, California 92679-
2025, USA

^c Institut Charles Gerhardt, AIME, UMR 5253 CNRS, Université Montpellier II, cc015
34095 Montpellier Cedex 5, France

Various top-down, bottom-up and hybrid fabrication routes of discontinuous palladium nano and mesostructures can be used for the fabrication of resistor based H₂ sensing devices. 1-D, 2D, and 3-D structures can be achieved using appropriate material templating and self-organization methods. Sensing mechanism is based on reversible gap closing/opening under H₂/H₂-free atmospheres undergoing the conversion equilibrium between Pd and PdH_{0.7}. Sensing performances depend on device designs and material microstructures and assembling/organizations.

Introduction

Resistive based hydrogen sensing usually involves the reversible conversion of palladium (Pd) into palladium hydride (PdH_{0.7}). This chemical conversion induces a resistivity change while the sensitive material changes from metal to semi-metal state in presence of hydrogen (1). H₂ sensing relies on the measurement of the resistivity changes in the palladium based material, as film, membrane or wire in presence of hydrogenated gas (2). Quantitative sensing is technically achievable since partial conversion induces a proportional increase in the resistivity. The limited signal changes, at the best by a factor of 1.8, however limit sensing performances (1).

Palladium to palladium hydride conversion also induces an increase by 11% of the molar volume of the pristine material. For a sensitive material based on isolated grains (ie without any electrical contact with closest neighbors – open circuit) and inter-grain distances in average less than 11% of grain volume, the volume increase undergoing the hydride formation, should theoretically close a certain number of break junctions in between grains generating electrical conductive paths through the material (closed circuit). In such H₂ switches system, despite an increase of the intrinsic resistivity of the material in semi-metal state (PdH_{0.7}) while originally metallic (Pd) in nature, closing gaps results in a large increase in the device conductivity, up to few orders of magnitude. Gap size distribution generates few or more conductive paths depending on the H₂ concentration in the measurement atmosphere, allowing quantitative measurements.

To validate this sensing approach, we have developed various top-down, bottom-up and hybrid fabrication routes of discontinuous palladium nano and mesostructures. These were assembled/organized on insulating surfaces for integration of resistor based devices for the specific sensing of H₂.

Results and Discussion

Top-down route: A single nanotrench in an evaporated palladium microwire

The selected top-down engineering approach explores advantages and limits of the use of reliable, repeatable and scalable lithography -based fabrication method for the perfect control of the number and the geometrical arrangement of nanogaps between two electrodes. A large set of material deposition techniques is available while the choice of the most suitable substrate is expected to simultaneously improve sensing performances and facilitate system integration procedures (3).

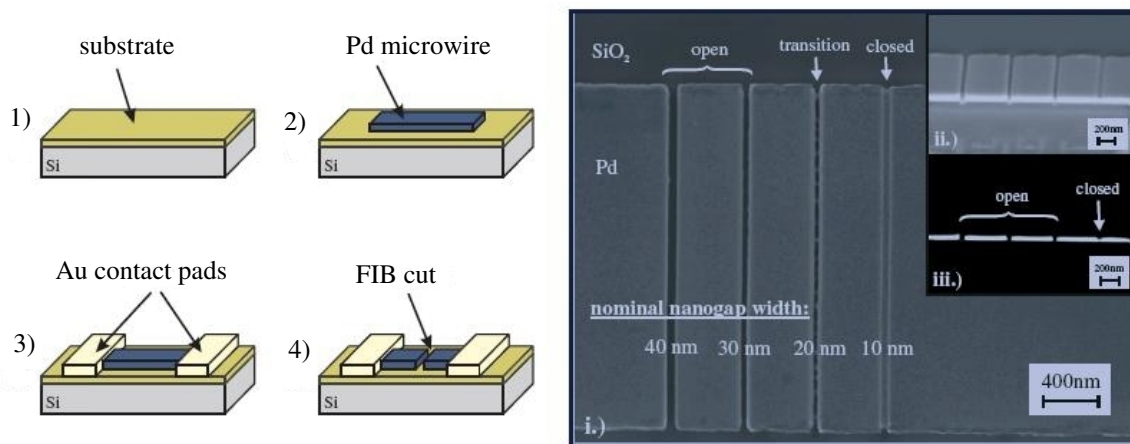


Figure 1. Left: Schematic process flow for fabrication of the sensing devices. Right: Analysis of four exemplary nanotrenches by SEM. (i) FIB cuts with different nominal widths (from left to right: 40, 30, 20, 10 nm) in a 50 nm thin Pd microwire, (ii) FIB milled cross section of the same trenches, (iii) the same image but with enhanced contrast. The images show open cuts, a partially open cut and a cut on the onset of milling.

Palladium microwires were fabricated by e-beam evaporation at room temperature and lift-off process (figure 1-left). The length of the wires is $85\mu\text{m}$ with a width of $2.8\mu\text{m}$ and different material thicknesses: 10, 25, 50 and 100 nm. Serving as electrical contacts, Au electrode pads were evaporated by shadow mask deposition. Two different insulating layers were used as substrates: (i) a thermal wet SiO_2 as a rigid layer, and (ii) a thick coating of polyimide (PI) as an elastic layer.

A single nanotrench has been fabricated by focused ion beam milling (FIB) in evaporated palladium microwires using an FEI Nova 600 NanoLab FIB workstation. Trenches of four different nominal widths (10, 20, 30 and 40 nm) were milled into wires of various thicknesses. As shown in Figure 1-right, the width of the trenches was estimated using scanning electron microscopy (SEM). Single FIB cuts were performed using milling doses in the range of $1\text{--}2\text{ (nm}^2\text{s)}^{-1}$ and $1.7\text{--}2.7\text{ (nm}^2\text{s)}^{-1}$. Doses were adjusted to completely open gaps in air.

Microwires on SiO_2 peeled off after a few H_2/N_2 cycles. These damages are caused by the high mechanical stress, on the order of several Gpa, induced by the Pd to PdH_x conversion in the thin microwire (4). In contrast, on PI substrate both 25 and 50nm thick wires showed closing effects under H_2/N_2 atmospheres. For 10nm thick wire, despite a PI Young's modulus of approximately 8.5 Gpa, the stress induced at the metal-polymer

interface still does not relax sufficiently to allow a complete lattice expansion to close the trench. The 100nm thick wire was not completely cut by FIB for the considered trench widths due to the required high aspect ratio. Increasing nominal widths resulted in large trenches which could not close even at 100% H₂.

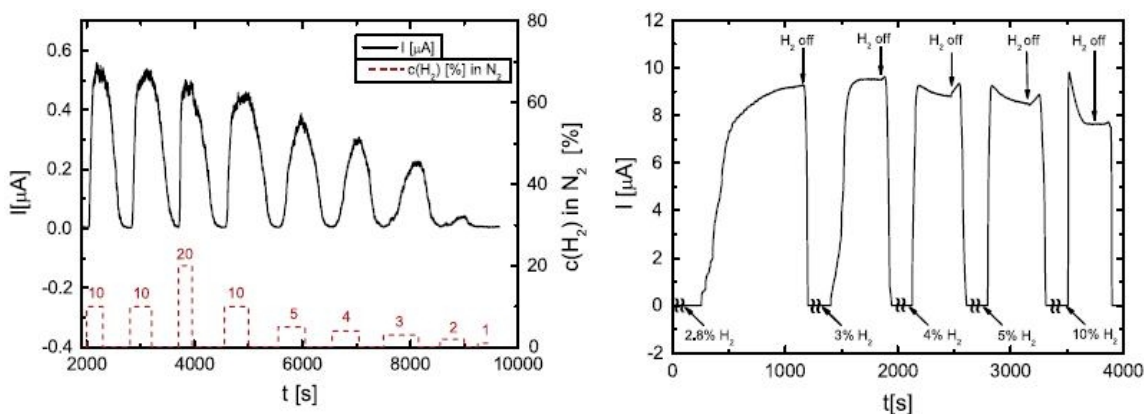


Figure 2. Typical electrical signal of FIB-cut Pd microwires on PI coating and a single nanotrench under various H₂/N₂ cycles (room temperature, bias = 20 mV). Left: 25 nm thick Pd wire, trench width: 61nm±5nm. Right: 50nm thick Pd wire, trench width: 26nm±5nm. The superposition of the mechanical closing of the gap (resulting in an increase in current) and the change in resistance due to the conversion of Pd to PdH_x (resulting in a decrease in current) become visible at H₂ concentrations above 3%. No response was observed for H₂ concentrations below 2.5%.

A typical electrical signal during H₂/N₂ cycles at different concentrations is shown in figure 2-left for a 25 nm thick Pd wire and 2-right for a 50 nm thick Pd wire both with a 1.5 nm thin Ti adhesion layer on PI. Trenches are respectively 61nm±5nm and 26nm±5nm in width. For samples with large trenches, sensing signal could accurately be fitted in a large H₂ concentration range with a classical Boltzmann function from which various characteristic parameters could be extracted including delay time. For smaller gap samples, the delay time was shortened and the electrical signal revealed the superposition of chemical and mechanical effects within sensing signal (over-shoot after H₂ closing in Figure 2-right: the mechanical closing of the trench and the chemical conversion of Pd to PdH_x (5)).

In situ atomic force microscopy (AFM) measurements confirmed that, in the presence of H₂, the trench closes and electrically connects the initially separated parts of the wire.

The thickness of the wire also influences the sensor behavior. First, the influence of the adhesion on the mechanical expansion decreases with the distance to the surface. The thicker the wire, the weaker the influence of the surface. Second, it determines the time needed for full hydride conversion: the thinner the wire, the faster the Pd to PdH_x conversion.

Bottom-up approach: Electrochemical synthesis and 1D and 3D palladium particles assemblies for H₂ detection

Electrodeposited Arrays of Palladium and Silver-palladium Mesowires. Arrays of palladium or silver-palladium mesowires have been obtained by electrochemical decoration of step-edges present at pyrolytic polycrystalline surfaces (HOPG) (6, 7).

Arrays have then been transferred onto a non-conductive substrate. Palladium and silver-palladium mesowire arrays were operated as H₂ sensor by applying a constant voltage of a few mV between evaporated gold contacts and measuring the corresponding 1–20 μ A current. As shown in Figure 3, the resistance of the sensor decreased in the presence of H₂. This decrease was related to H₂ concentration, with a proportional detection in the range from 12 to 0.5% H₂ in N₂ for pure palladium-based sensor.

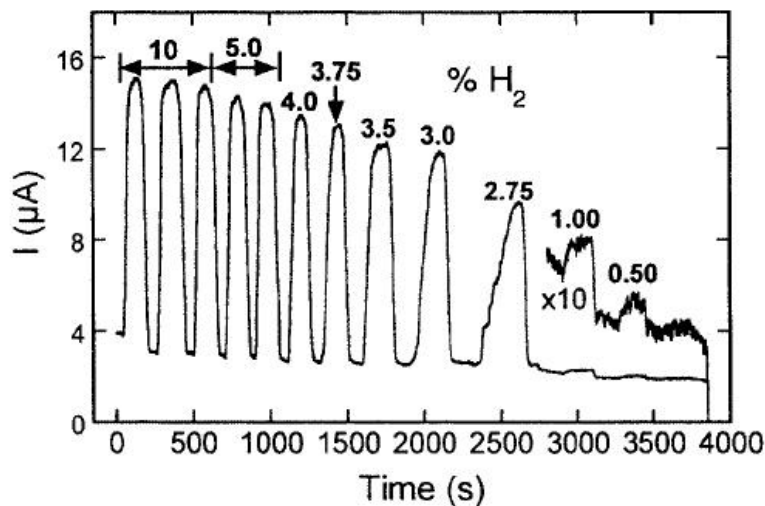


Figure 3. Current response of a palladium mesowire-based H₂ sensor under exposure to hydrogen/nitrogen mixtures (concentration of H₂ as shown).

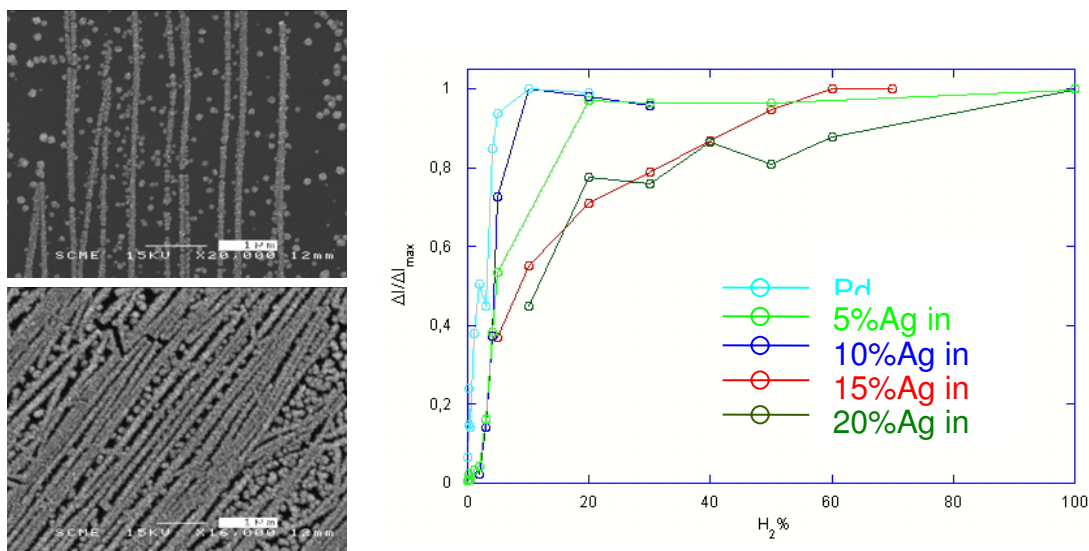


Figure 4. SEM micrographies of Pd-Ag mesowires at 15%Ag in Pd (top-left) and 20%Ag in Pd (bottom-left) electrodeposited for 300s respectively at 0.32V/Ag-AgCl and 0.29V/Ag-AgCl. On the right, relative current changes versus H₂/N₂ concentration measured for a 20mV bias for sensors built from Pd-Ag mesowires of various alloy compositions (given in the graph).

In contrast to existing resistor-based H₂ sensors, however, the resistance of our mesowire-based sensors decreased in the presence of H₂. The mechanism that we propose

to account for this 'inverse' response has been confirmed using AFM: before any initial exposure to H_2 , the sensor showed a measurable value for the resistance in air. At this stage, the nanowire array includes continuous as well as broken wires. Under a hydrogen atmosphere, palladium metal converts into the thermodynamically stable $PdH_{0.7}$. The subsequent increase in the lattice volume (11% at 25°C with 1.0 atm H_2) closes some nanoscopic gaps along these wires. It is the closing of these 'break junctions' that accounts for the decreased resistance of the sensor in opposition to the increased resistivity of palladium hydride relative to palladium. Exposure back to air opens these gaps in mesowires in the sensor. The motion of mesowire segments responsible for the reversible and reproducible break junctions is the direct result of the swelling of individual palladium grains in the presence of H_2 . Perfectly suited for safety purpose, the limited detection range from 12 to 0.5% H_2 in N_2 has been extended to full concentration range from 0.5 to nearly 100% using mesowires made of PdAg alloys of various compositions (Figure 4).

Disorganised Palladium Particles 3D Assemblies for H_2 Detection. Back in 2006, in the same time frame as Zamborini (8), we have developed a new bottom-up approach for the fabrication nanoparticle-based H_2 sensors.

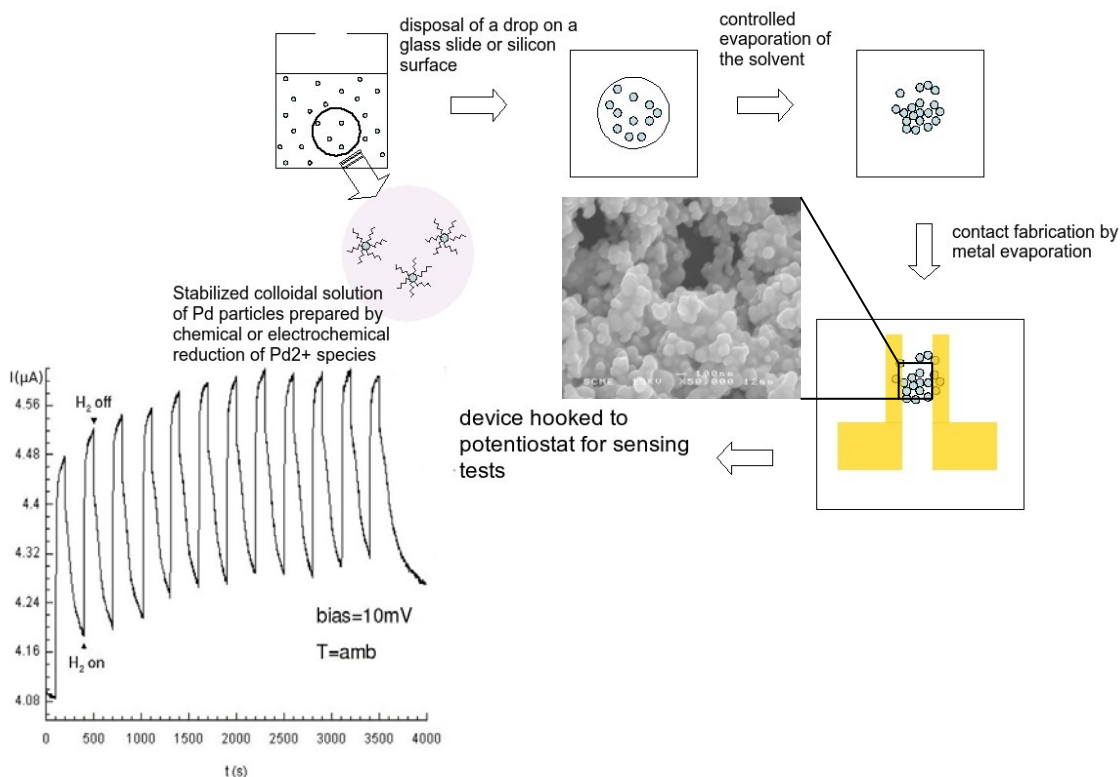


Figure 5. Process-flow for the fabrication of Pd particle-based H_2 sensor from electrogenerated colloid and electrical sensing signal under 5% H_2/N_2 flux for 100s.

In this approach, palladium nanoparticles were electrochemically generated by reduction of an anhydrous metal salt solubilized in a polar organic medium. This preparation method developed by Reetz is perfectly suited for the preparation of stable metal colloids (9). An alkylammonium surfactant simultaneously acts as electrolyte support as well as colloid stabilizer. Concentrated Pd colloids are obtained by

electrochemical reduction under controlled atmosphere of a Pd salt (4mM PdCl₂) in 0.1M tetraoctylammoniumbromide/dry THF electrolyte. Ad-atoms generated at the cathode form small clusters which are quickly stabilized by the cataionic surfactant. Particle size from 2 to 10nm can be tuned by controlling the applied current density (in the range of a few mAcm⁻²). The larger the current density, the smaller the particles. By slow evaporation of the solvent, micro-sized aggregates were deposited onto a glass or silicon surface. Device integration was achieved using metal contacts obtained by sputtering through a designed stencil mask allowing electrical measurements. The whole process-flow is summarized in Figure 5 together with the typical electrical response of a sensor under 5% H₂ in N₂ mixture.

Hybrid approach: Surface organization of overgrown palladium islands with nanoscale gap separations.

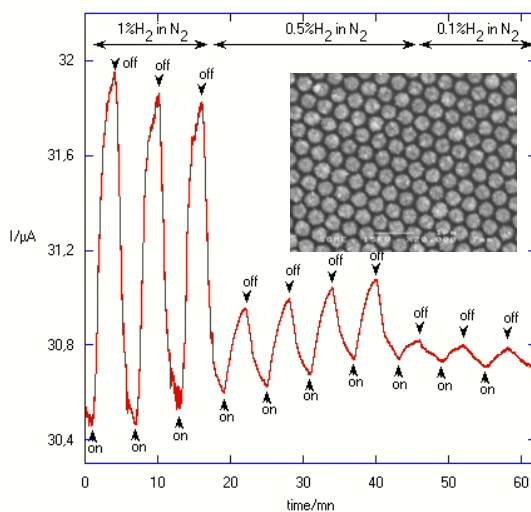


Figure 6. Response of a Pd island based sensor fabricated by hybrid approach (20mV bias) at low concentrations of H₂ in N₂ and SEM micrography of the sensitive part.

This hybrid route proceeds by electrochemical deposition of palladium islands on highly doped N-type silicon through a pre-patterned insulating layer (10). Surface patterning is achieved through the fabrication of a lithographically engineered insulating layer onto the electrode surface. Template design consists in 2D hexagonal arrangement of holes through an insulating layer with nominal inter-hole distances and hole diameters in the range of few tens of nanometers. Pd electrodeposition has been performed for a controlled overgrowth at the insulator surface while keeping few nanometer gap separations from islands to islands. A 2-4mM PdCl₂ aqueous solution in hydrochloric electrolyte is used to perform this electrochemical step. Gold contacts are evaporated through metal masks to allow sensing measurements. Figure 6 shows a SEM image of the sensing surface as insert of the current response vs time of the corresponding sensor under H₂/N₂ flows at low H₂ concentrations. Detection signal is proportional in a large concentration range from 0.1% to 50% of H₂ in N₂ due to the gap size distribution arising from the high surface roughness of polycrystalline Pd islands obtained using these electrolysis parameters. As for sensors fabricated by other bottom-up or top-down approach, measured response and recovery times are fast and sensors can be cycled over a large number of H₂/H₂-free cycles.

Conclusion

We have developed various top-down, bottom-up and hybrid fabrication routes of H₂ sensors based on discontinuous palladium nano and mesostructures. These routes tends to optimize the sensitive part design especially surface organization, mesostructure and gap sizes, mesostructure chemical composition, and mechanical properties of the substrate. These various parameters strongly impact on H₂ sensing performances.

Acknowledgments

Authors would like to acknowledge the technical support from the Center of MicroNanotechnology (CMI) in Lausanne and Michel Ramonda from LPCP (Laboratoire de Microscopie en Champ Proche), UM-II in Montpellier, for AFM measurements under hydrogen. Financial support from the FP6 Integrated Project HySYS SES6-019981 and from Peugeot-Citroen-Automobile (PCA) is gratefully acknowledged. Parts of this project have been developed within the frame-works of two international exchange programs co-funded by NSF and CNRS (UC Irvine – Université Montpellier 2 collaboration) and Swiss and French governments through Germaine de Stael program (Ecole Polytechnique Fédérale de Lausanne – Université Montpellier 2 collaboration)

References

1. F. A. Lewis, in *The Palladium Hydrogen System*, Academic Press, New York (1967).
2. F.J. DiMeo and B. Chen, *Proc. 2000 DOE Program Rev.*, U.S. Department of Energy (2000).
3. T. Kiefer, F. Favier, O. Vazquez-Mena, G. Villanueva, and J. Brugger, *Nanotechnology*, **19**, 125502 (2008).
4. U. Laudahn, S. Faehler, H.U. Krebs, A. Pundt, M. Bicker, U.V. Huelsen, U. Geyer, and R. Kirchheim, *Appl. Phys. Lett.*, **74**, 647 (1999).
5. J.E. Morris, A. Kiesow, M. Hong, and F. Wu, *Int. J. Electron.*, **81**, 441 (1996).
6. F. Favier, E. Walter, T. Benter, and R.M. Penner. *Science*, Sept 21, 2227 (2001).
7. E. Walter, F. Favier, and R.M. Penner. *Analytical chemistry*, **74**, 1546 (2002).
8. F.J. Ibanez and F.P. Zamborini, **22**, 23, 9789 (2006).
9. M.T. Reetz and M. Maase, *Adv. Mater.*, **11**, 9, 773 (1999).
10. F. Favier, J. Brugger, and J.-F. Ranjard, French patent application #0757673, 09/19/2007.